Earthquakes and Structures, *Vol. 17, No. 1 (2019) 17-29*
DOI: https://doi.org/10.12989/eas.2019.17.1.017

Blast-load-induced interaction between adjacent multi-story buildings

Sayed Mahmoud*

Department of Civil and Construction Engineering, College of Engineering, Imam Abdulrahman Bin Faisal University, Dammam, Saudi Arabia

(Received February 3, 2019, Revised April 8, 2019, Accepted April 10, 2019)

Abstract. The present study aims to present a comprehensive understanding of the performance of neighboring multi-story buildings with different dynamic characteristics under blast loads. Two different scenarios are simulated in terms of explosion locations with respect to both buildings. To investigate the effect of interaction between the neighboring buildings in terms of the induced responses, the separation gap is set to be sufficiently small to ensure collisions between stories. An adequately large separation gap is set between the buildings to explore responses without collisions under the applied blast loads. Several blast loads with different peak pressure intensities are employed to perform the dynamic analysis. The finite-element toolbox Computer Aided Learning of the Finite-Element Method (CALFEM) is used to develop a MATLAB code to perform the simulation analysis. The dynamic responses obtained in the scenarios considered herein are presented comparatively. It is found that the obtained stories' responses are governed mainly by the location and intensity of the applied blast loads, separation distances, and flexibility of the attacked structures. Moreover, explosions near a light and flexible building may lead to a significant decrease in blast resistance because explosions severely influence the dynamic responses of the building's stories.

Keywords: explosive loads; adjacent structures; separation gaps; pounding forces

1. Introduction

Recently, intentional or accidental explosions have emerged as the most severe man-made hazards for both civil and military structures. As such, there is a need to investigate the dynamic response of civilian and military structures to protect them from explosive events. The pressure loading generated by explosives is very complex and is highly affected by several factors, including the type and size of explosive, distance between explosive and structure, and existence of objects in the distance between explosive and structure.

Investigating the response of structures to dynamic blast loads via experimental studies is difficult because the experimental equipment must be modified to achieve the desired high temporal and spatial resolution during the short loading time. Owing to such complications in terms of equipment modification and short duration of applied dynamic load, experimental works cannot facilitate deep exploration of structural responses under explosive loads. Numerical simulation is another strategy for analyzing the dynamic responses of structures to explosive loads. Blast investigation by employing numerical simulation together with experimental study is called the coupled approach.

For protecting structures against sudden explosive loads, several studies have focused on the effect of explosives on reinforced concrete (RC) and steel buildings. Most of these studies investigated the response of an individual structural element, such as beams, columns, or walls, by employing the aforementioned experimental and numerical strategies. Zhang *et al*. (2013) performed an experimental study to investigate the damage to small-scale RC beams exposed to different explosives. Yao *et al*. (2016) studied the influence of two different stirrup ratios on the induced dynamic response and damage characteristics of two sets of specimens of RC beams by performing experimental and numerical analysis. Moreover, the numerical approach has been employed successfully to simulate the response of RC members subjected to explosive blast loads. Bao and Li (2010) employed the numerical approach to investigate the dynamic behavior of RC columns subjected to short standoff blast loads by using a finite-element (FE) model. Elsanadedy *et al*. (2014) conducted a simplified nonlinear dynamic analysis to assess the vulnerability of a typical steel building to a terrorist attack by using the FE package LS-DYNA. Jain *et al*. (2015) utilized the FE technique to investigate the dynamic response of a RC wall to blast loading by considering the effect of several parameters, such as wall thickness, grade of concrete, and steel reinforcement. Yan *et al*. (2015) introduced a robust technique based on the arbitrary-Lagrange-Euler approach to simulate the explosive loads acting on small-scale RC beams. Kumar *et al*. (2010) used a simplified blast-load model to perform dynamic analysis of a semi-buried steel structure subjected to explosive loads of different magnitudes and standoff distances to investigate the deflection and von Mises stress at the center of the plate. Similarly, Dyer *et al*. (2018) used the simplified blast model with only the forced vibration phase to examine the lateral behaviors of tanks under accidental industrial explosive loads. Mahmoud (2014) performed numerical simulations to study the effects of soil flexibility on the dynamic

*Corresponding author, Ph.D.
E-mail: elseedy@hotmail.com

 ISSN: 2092-7614 (Print), 2092-7622 (Online)

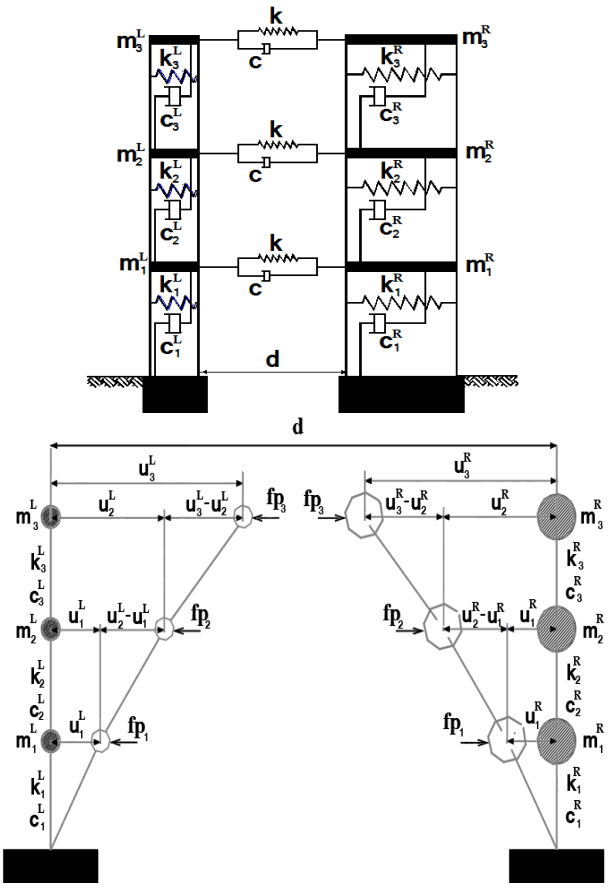

Fig. 1 MDOF building model of adjacent buildings

responses of structures under typical explosive loads, together with the associated structural damage.

The present study aims to investigate the dynamic response of adjacent structures subjected to blast loadings with different peak pressures by using a purpose-built MATLAB code. The code uses the step2 function embedded in the FE toolbox Computer Aided Learning of the Finite-Element Method (CALFEM). The buildings are modeled with multiple degrees of freedom (MDOF) and different dynamic characteristics. Two different scenarios are analyzed in terms of the separation gap between adjacent buildings. Moreover, two different explosion positions are considered to study their influence on induced responses and damage level to the building stories. The effect of variation in peak pressures on the induced story responses is studied as well.

2. Building model

Herein, the focus is on the dynamic behavior of sufficiently and insufficiently separated buildings subjected to dynamic explosive loads. The dynamic behavior of the building models is investigated without and with consideration of the effect of collisions under applied dynamic loads. The considered building models are characterized by their masses lumped at the floor levels. A nonlinear viscoelastic model is incorporated at each floor level to capture the induced pounding force during collisions for the insufficiently separated case.

3. Governing equations of motion

This section presents the coupled equations of motion of the building models shown in Fig. 1 considering and ignoring the effect of collisions during application of dynamic explosive loads.

3.1 Equations of motion ignoring collision

The dynamic equation of motion of the structural models ignoring collisions can be written as follows

$$\begin{pmatrix} M^L & O \\ O & M^R \end{pmatrix}\begin{pmatrix} \ddot{U}^L \\ \ddot{U}^R \end{pmatrix} + \begin{pmatrix} C^L & O \\ O & C^R \end{pmatrix}\begin{pmatrix} \dot{U}^L \\ \dot{U}^R \end{pmatrix} + \begin{pmatrix} K^L & O \\ O & K^R \end{pmatrix}\begin{pmatrix} U^L \\ U^R \end{pmatrix} = \begin{pmatrix} F^L \\ F^R \end{pmatrix} \quad (1)$$

where $\boldsymbol{M}^L$, $\boldsymbol{C}^L$, $\boldsymbol{K}^L$ and $\boldsymbol{M}^R$, $\boldsymbol{C}^R$, K^R denote the masses, damping, and stiffness matrices for the left and right buildings, respectively; $\boldsymbol{U}^L$, $\dot{\boldsymbol{U}}^L$, $\ddot{\boldsymbol{U}}^L$ and $\boldsymbol{U}^R$, $\dot{\boldsymbol{U}}^R$, $\ddot{\boldsymbol{U}}^R$ are vectors representing the displacement, velocity, and acceleration for the left and right structures, respectively; and $\boldsymbol{F}$is the vector of the applied explosive loads.

The elements of the aforementioned matrices in terms of story mass m_i^L, m_i^R; damping c_i^L, c_i^R; and stiffness coefficients k_i^L, k_i^R (i=1, 2, 3) for the left and right buildings, respectively, can be expressed as follows

$$\boldsymbol{M}^L = \begin{pmatrix} m_1^L & 0 & 0 \\ 0 & m_2^L & 0 \\ 0 & 0 & m_3^L \end{pmatrix},\ \boldsymbol{M}^R = \begin{pmatrix} m_1^R & 0 & 0 \\ 0 & m_2^R & 0 \\ 0 & 0 & m_3^R \end{pmatrix}, \quad (2a)$$

$$\boldsymbol{O} = \begin{pmatrix} 0 & 0 & 0 \\ 0 & 0 & 0 \\ 0 & 0 & 0 \end{pmatrix},$$

$$\boldsymbol{C}^L = \begin{pmatrix} c_1^L + c_2^L & -c_2^L & 0 \\ -c_2^L & c_2^L + c_3^L & -c_3^L \\ 0 & -c_3^L & c_3^L \end{pmatrix},$$

$$\boldsymbol{C}^R = \begin{pmatrix} c_1^R + c_2^R & -c_2^R & 0 \\ -c_2^R & c_2^R + c_3^R & -c_3^R \\ 0 & -c_3^R & c_3^R \end{pmatrix}$$

$$K^L = \begin{pmatrix} k_1^L + k_2^L & -k_2^L & 0 \\ -k_2^L & k_2^L + k_3^L & -k_3^L \\ 0 & -k_3^L & k_3^L \end{pmatrix},$$

$$K^R = \begin{pmatrix} k_1^R + k_2^R & -k_2^R & 0 \\ -k_2^R & k_2^R + k_3^R & -k_3^R \\ 0 & -k_3^R & k_3^R \end{pmatrix} \quad (2b)$$

Similarly, the elements of the vectors in terms of the story displacements u_i^L, u_i^R; velocity $\dot{u}_i^L$, $\dot{u}_i^R$; and acceleration $\ddot{u}_i^L$, $\ddot{u}_i^R$ can be defined as follows:

$$\boldsymbol{U}^L = \begin{pmatrix} u_1^L \\ u_2^L \\ u_3^L \end{pmatrix},\ \dot{\boldsymbol{U}}^L = \begin{pmatrix} \dot{u}_1^L \\ \dot{u}_2^L \\ \dot{u}_3^L \end{pmatrix},\ \ddot{\boldsymbol{U}}^L = \begin{pmatrix} \ddot{u}_1^L \\ \ddot{u}_2^L \\ \ddot{u}_3^L \end{pmatrix}, \quad (2c)$$

$$\boldsymbol{U}^R = \begin{pmatrix} u_1^R \\ u_2^R \\ u_3^R \end{pmatrix},\ \dot{\boldsymbol{U}}^R = \begin{pmatrix} \dot{u}_1^R \\ \dot{u}_2^R \\ \dot{u}_3^R \end{pmatrix},\ \ddot{\boldsymbol{U}}^R = \begin{pmatrix} \ddot{u}_1^R \\ \ddot{u}_2^R \\ \ddot{u}_3^R \end{pmatrix} \quad (2d)$$

The right-hand side vectors F^L and F^R refer to the explosive loads that attack the left and the right buildings, respectively. The pressure p_i and the equivalent areas A_i^L and A_i^R of the left and right buildings, respectively, can be used to define the explosive loads on the right-hand side as follows

$$F^L = \begin{pmatrix} p_1 A_1^L \\ p_2 A_2^L \\ p_3 A_3^L \end{pmatrix},\ F^R = \begin{pmatrix} p_1 A_1^R \\ p_2 A_2^R \\ p_3 A_3^R \end{pmatrix} \tag{2e}$$

3.2 Equations of motion considering collision

The equations of motions in (1) are not coupled and can be solved separately. However, during collisions, the equations of motions are coupled through the induced pounding forces at the story levels of adjacent building structures. The vector F_p that contains the impact forces acts as the coupling term of the equations of motions given in (3)

$$\begin{pmatrix} M^L & 0 \\ 0 & M^R \end{pmatrix}\begin{pmatrix} \ddot{U}^L \\ \ddot{U}^R \end{pmatrix} + \begin{pmatrix} C^L & 0 \\ 0 & C^R \end{pmatrix}\begin{pmatrix} \dot{U}^L \\ \dot{U}^R \end{pmatrix} + \begin{pmatrix} K^L & 0 \\ 0 & K^R \end{pmatrix}\begin{pmatrix} U^L \\ U^R \end{pmatrix} + \begin{pmatrix} Fp \\ -Fp \end{pmatrix} = \begin{pmatrix} F^L \\ F^R \end{pmatrix} \tag{3}$$

The elements of the pounding force vector at each story level i, (i=1,2,3) can be written as follows

$$Fp = \begin{pmatrix} fp_1 \\ fp_2 \\ fp_3 \end{pmatrix}, \tag{4}$$

The value of f_{pi} at each story level can be calculated using Eq. (5).

3.3 Solution procedure for equations of motion

Eqs. (1) and (3) are solved numerically by using the FE toolbox CALFEM. The function 'step2' in the toolbox is used to perform integration at the time interval specified by the user. The developed function uses the step-by-step Newmark family methods with constant coefficients γ and β, which can be set by the user. The average acceleration approach is employed herein with γ=0.5 and β=0.25 over a small-time interval to achieve unconditional stability.

4. Nonlinear model for pounding simulation

Several models can be used to study the problem of interaction between insufficiently separated structures under dynamic loads. Some of these models only applies a linear or nonlinear elastic spring ignoring the dissipated energy during contact (Maison and Kasai 1992, Chau and Wei 2001). Some other models have been proposed with linear spring in conjunction with a linear dashpot to account for some of the dissipated energy during collisions (Anagnostopoulos and Spiliopoulos 1992). However, these models have been found to produce a negative force due to impact just before separation. Among the available models for capturing impact between insufficiently separated buildings subjected to dynamic load, the nonlinear viscoelastic model is used herein. Nonlinear impact spring and dashpot elements are used in the utilized nonlinear model to capture the induced impacts at each story level of the adjacent buildings. Impacts at the i^{th} (i=1,2,3) story level can be estimated according to Jankowski (2005) as follows

$$\begin{aligned} fp_i &= \bar{\beta}\delta_i^{\frac{3}{2}} + \bar{c}_i\dot{\delta}_i && \text{for } \delta_i > 0 \text{ and } \dot{\delta}_i(t) > 0 \\ fp_i &= \bar{\beta}\delta_i^{\frac{3}{2}} && \text{for } \delta_i > 0 \text{ and } \dot{\delta}_i(t) \le 0 \\ fp_i &= 0 && \text{for } \delta_i \le 0 \end{aligned} \tag{5}$$

where $\delta_i = (u_i^l - u_i^r - d)$ and $\dot{\delta}_i(t) = (\dot{u}_i^l - \dot{u}_i^r)$ are the relative displacement and velocity between the colliding i^{th} stories, respectively; d denotes the gap between adjacent buildings; and $\bar{\beta}$ is a parameter that defines impact stiffness. The damping coefficient $\bar{c}_i$ of the impact element can be defined in terms of the masses of the colliding stories, relative displacement, damping ratio of the impact element $\bar{\xi}$, and the impact stiffness parameter $\bar{\beta}$ as follows

$$\bar{c}_i = 2\bar{\xi}\sqrt{\bar{\beta}\sqrt{\delta_i}\frac{m_i^l m_i^r}{m_i^l + m_i^r}}. \tag{6}$$

The value of the impact damping ratio $\bar{\xi}$ can be estimated in terms of the coefficient of restitution, e as follows (2006)

$$\bar{\xi} = \frac{9\sqrt{5}}{2}\frac{1-e^2}{e(e(9\pi-16)+16)}. \tag{7}$$

5. Air blast-load profile

An explosion causes a sudden energy release that results in what is called a pressure transient or a blast wave. These induced blast waves propagate from the source at supersonic speed in all directions. The nature of the released energy and the measured distance from the source of explosion are two key parameters that control the shape and magnitude of the created blast waves. The idealized air blast-wave profile of pressure due to the detonation of explosives with respect to time is presented in Fig. 2. As can be seen from the figure, the plotted idealized wave shows an almost instantaneous rise in pressure above the ambient pressure, as denoted by P_a, to the maximum

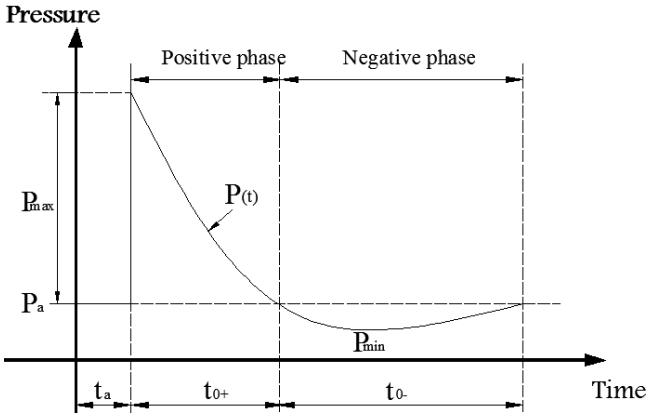

Fig. 2 Schematic representation of ideal explosion as a pressure time-history curve

incident overpressure $P_{\max}$. The assigned value of incident overpressure decays following an exponential pass to the atmospheric value during the positive phase duration t_{0+}. The suction or negative phase with duration t_{0-}, which follows the positive one, is usually longer than the positive phase and is characterized by the peak negative value $P_{\min}$. Kinny and Graham (1984) proposed a widely used exponential equation in terms of the durations of the positive and negative phases to describe the rate of decrease in blast pressure $P(t)$ at any time t as follows

$$P(t) = P_{max}(1 - \frac{t}{t_{0+}})e^{\left(-\frac{bt}{t_{0-}}\right)} \quad (8)$$

where the parameter b refers to the decay of the time-pressure curve.

Several formulae have been proposed to calculate the peak incident pressure P_{max}. Kinny and Graham (1984) introduced an extensively used formulation for computer calculation purposes based on scaled distance from the center of explosion d with respect to the mass of the explosive charge W as follows

$$P_{max} = \frac{808\, P_a \left[1+\left(\frac{Z}{4.5}\right)^2\right]}{\sqrt{1+\left(\frac{Z}{0.048}\right)^2}\sqrt{1+\left(\frac{Z}{0.32}\right)^2}\sqrt{1+\left(\frac{Z}{1.35}\right)^2}} \quad (9)$$

Baker *et al.* (1973) defined the scaled distance Z as follows

$$Z = \frac{d}{\sqrt[3]{W}} \quad (10)$$

Smith (1994) presented the following equation for evaluating the value of suction pressure $P_{\min}$, which is lower than the ambient pressure, as follows

$$P_{min} = \frac{0.35}{Z} 10^5 \text{ Pa} \qquad \text{for Z>1.6} \quad (11)$$

6. Damage model

From structural analysis and blast-resistant design point of view, damage can be evaluated and quantified in terms of a numerical damage index. The characteristics of an applied blast load, the induced dynamic response of a structure under a blast load and the results from the nonlinear dynamic analysis may affect the damage index as a measure of damage. The response-based damage index can be used to refer to the global damage of the whole structure or structural components such as horizontal elements in terms of beams or vertical elements in terms of columns. Damage index is a dimensionless parameter ranges between zero and one. The zero value refers to the state of undamaged structure and the one value is for the state of collapsed structure. The intermediate values indicate different levels of damages between the above-mentioned two states.

Several indices have been proposed to quantify the damage sustained by a structure under dynamic loading (Park and Ang 1985, Powell and Allahabadi 1988, Cosenza *et al.* 1993). The damage to a building subjected to an explosion is measured mainly by using the parameters related to the modeled system, and damage indices are based on the results of dynamic analyses. In addition to the key parameter of induced structural deformation, plastic

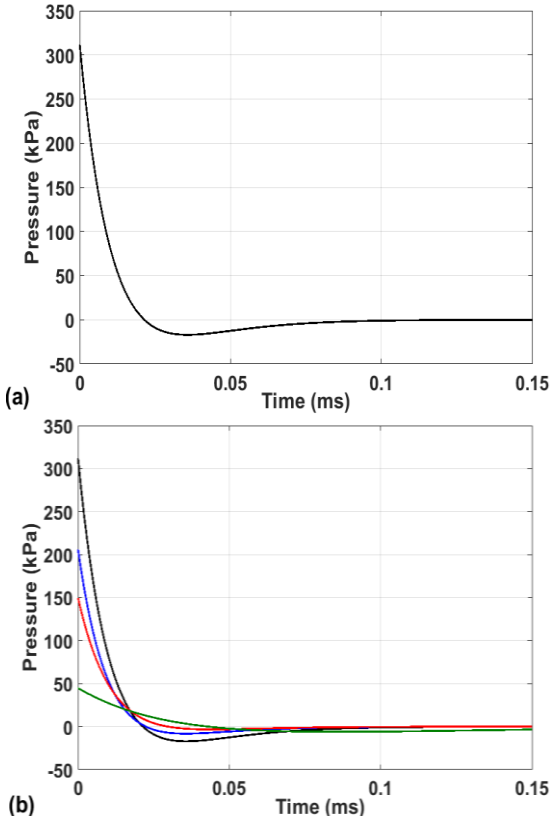

Fig. 3 (a) Single blast load and (b) various blast loads with different peak overpressures

energy is used to determine structural damage. One of the most commonly used damage indices is the one introduced by Park and Ang (1985). This index is expressed in terms of the induced maximum deformation and the absorbed hysteretic energy as follows

$$DI_{PA} = \frac{U_{max}}{U_u} + \alpha \frac{E_H}{F_y U_u} \quad (12)$$

where U_{max} represents the induced maximum displacement of a building model under an applied dynamic blast load, and U_u is the ultimate displacement of the system. Notably, the ultimate displacement can be computed based on yield displacement U_y and ductility μ as $U_u = \mu U_y$. The term α is a positive parameter that represents the effect of cyclic loading on structural damage. The hysteretic energy absorbed by the structure is denoted by E_H, and F_y is the yield strength of the structure.

7. Numerical results and discussion

In the current analysis, the blast loads shown in Fig. 3 were applied to the building model shown in Fig. 1. For comparison and to illustrate the effectiveness of the location of the applied explosive blast load, the dynamic responses of the building models were calculated by employing two approaches. The first approach involved using the typical blast-load model near the light and flexible building, while the second involved employing the blast-load model next to the heavier and stiff building model.

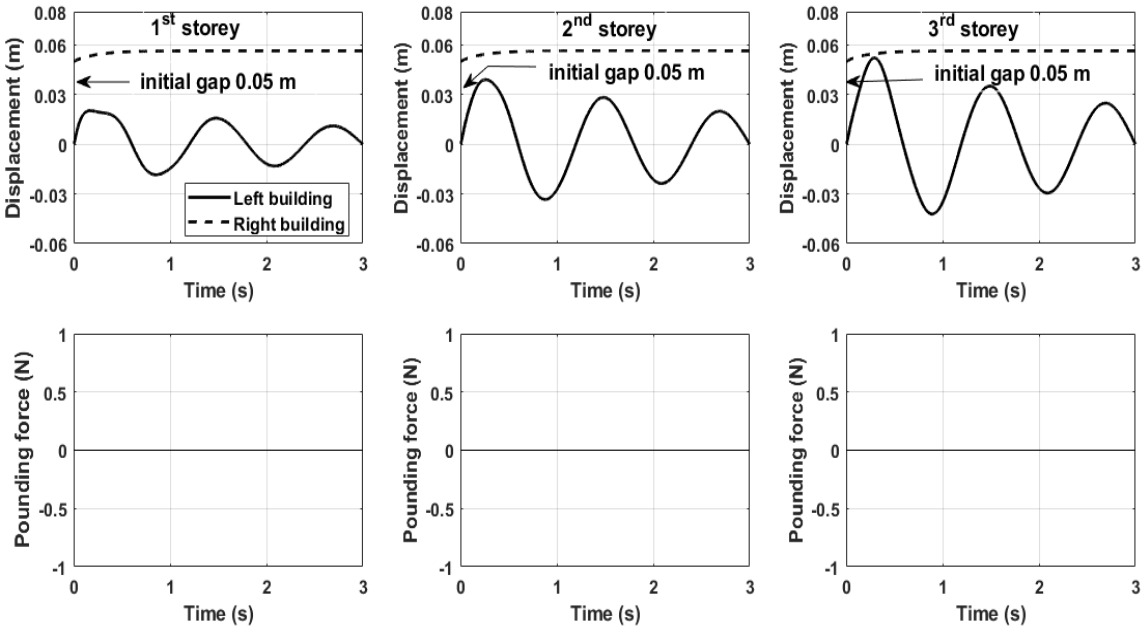

Fig. 4 Displacement and impact force time-histories of adjacent buildings with large separation gap to an explosion near flexible building

The pressure-time diagrams of the considered various blast loads were calculated and applied as time history functions to all the buildings masses. The equivalent areas of the lumped masses as well as the height of floors from the source of explosion affect the trnsmitted blast value acting at each floor level. First, the analyses were performed using the typical blast-wave profile shown in Fig. 3(a). The dynamic characteristics of the adjacent building models were mass of 25×10^3 kg for the flexible building and 1000×10^3 kg for the stiff building, damping ratio of 0.05, natural system period of 1.2 s and 0.3 s for the flexible and stiff buildings, respectively, and yield strength $f_y = 1.369 \times 10^5$ N/mm^2 $f_y = 1.442 \times 10^7$ N/mm^2 for the light and heavy buildings, respectively. The parameter α representing the effect of cyclic loading on structural damage was set to 0.15 (see Mahmoud 2016). The quantities of interest in terms of the calculated response were displacement, pounding force, and damage index, which could be obtained from the MDOF analysis performed following application of the two loading scenarios. The selected response quantities are especially important to structural designers because any induced structural displacement above a certain limit may damage the structural elements. In addition, the induced pounding forces may severely damage or even cause total collapse. The numerical simulations were extended to include blast loadings with different peak overpressures and positive durations (see Fig. 3(b)). The computed displacement, pounding force, and damage index due to the considered explosives are presented against the simulation time for the typical blast loads considered in the study. In addition, the peak displacements, peak pounding forces, and peak damage indices were calculated and are presented. As it is known that the value of separation gap is a function of the relative displacement between the neighbouring structures which in turn depends on the dynamic characteristics of these structures in terms of the natural periods and damping ratios (Lopez-Garcia and Soong 2009). The dynamic characteristics of the considered herein MDOF adjacent building models provide through simulation analysis separation gaps with values vary from 0 to 0.04 m to ensure collisions between stories of the considered adjacent buildings. For separation gap more than 0.04m, buildings move freely without impacting. The selected separation gap has been set to be of 0.01 m for pounding simulation case and 0.05m for the case of no pounding.

The responses and peak responses without and with consideration of neighboring building's collisions under the applied dynamic blast loads are addressed. The numerical results for the effect of separation gap as an influential parameter on the induced responses and the maximum responses are calculated and presented in the following subsections. In addition, the results obtained by varying the peak over static pressure values on the induced dynamic responses are numerically simulated and presented.

7.1 Single blast load

The previously described typical blast-load model (see Section 2) with $p_{\max} = 206$ kPa, $t_0 = 0.02242$ ms, and $b = 1.701$ was used to perform dynamic analyses of neighboring buildings with MDOF, as illustrated in Fig. 1, with variable separation distance. The computed story response time-histories in terms of displacements and forces due to collisions under dynamic blast load next to the flexible building model are presented in Figs. 4 and 5, respectively. Fig. 4 presents the results for the state in which the separation gap was sufficiently large to prevent collisions between the two building models. The trend in the displacement response results of the stories of the light and flexible building shows a substantial change with variations in simulation time. However, the trend observed

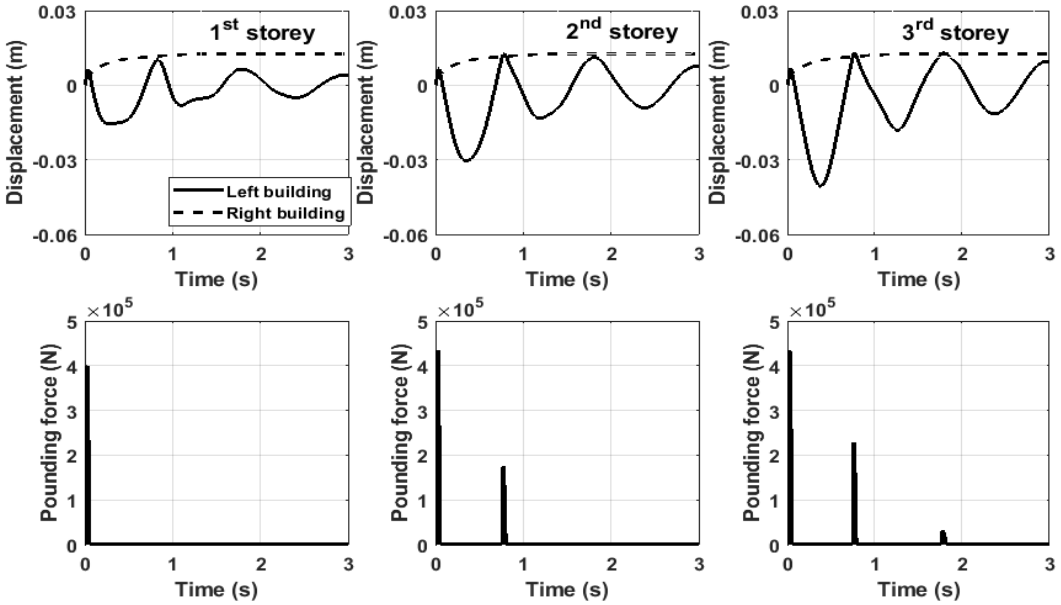

Fig. 5 Displacement and impact force time-histories of adjacent buildings with small separation gap to an explosion near flexible building

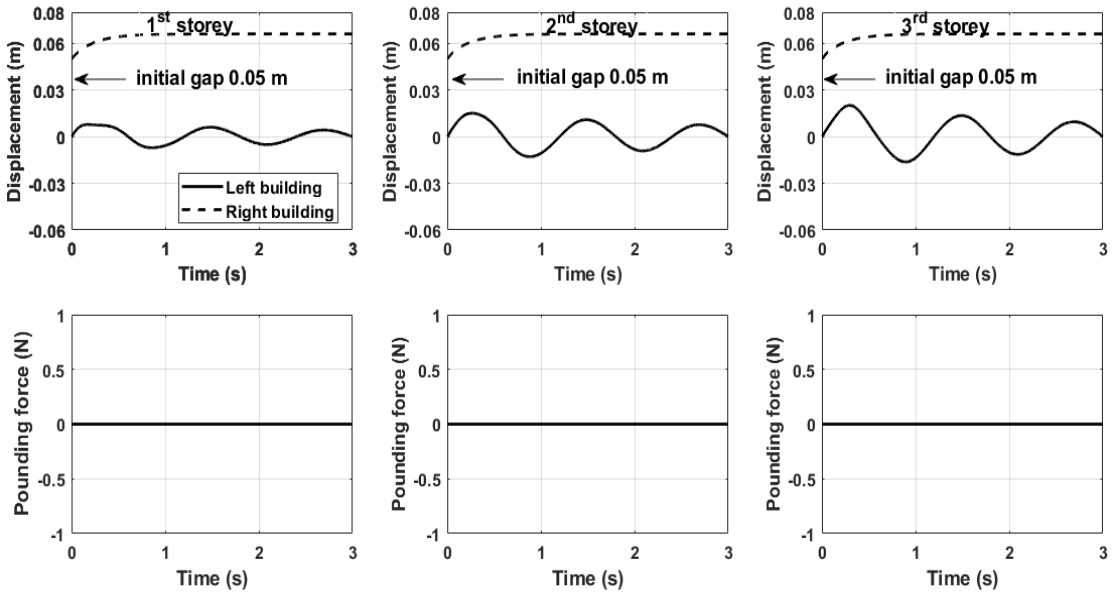

Fig. 6 Displacement and impact force time-histories of adjacent buildings with large separation gap to an explosion near stiff building

in case of the stiff and heavy building shows nearly unchanged values with time. Based on an analysis of the results, the simulated and measured displacement time-histories of the 1st, 2nd, and 3rd stories of the left building are 0.020 m, 0.039 m, and 0.052 m, respectively. The peak displacement induced in the 1st, 2nd, and 3rd stories of the stiff and heavy right building is 0.004 m. The state in which the provided separation gap between the neighboring buildings is set to be small enough in order to ensure collisions between the stories of adjacent buildings is presented in Fig. 5. The figure clearly indicates that considering the effects of these potential impacts on the induced story displacements leads to a considerable decrease in story displacements of the light and flexible building to 0.016 m, 0.030 m, and 0.041 m for the 1st, 2nd, and 3rd stories, respectively, as compared to the induced story displacement results of the state without collisions. By contrast, a comparison of the captured displacement results of the stories of the right and stiff building due to collisions with the corresponding values of the case without collisions shows an increase in the induced story displacements. Moreover, the figure shows that the obtained displacements of the stories of the stiff building under the applied explosive load are almost the same. For the insufficiently separated building models, the figure clearly shows that the explosion induces impact forces at all considered story levels. In addition, the first peak impact force occurs immediately after the explosion. Moreover, the explosion

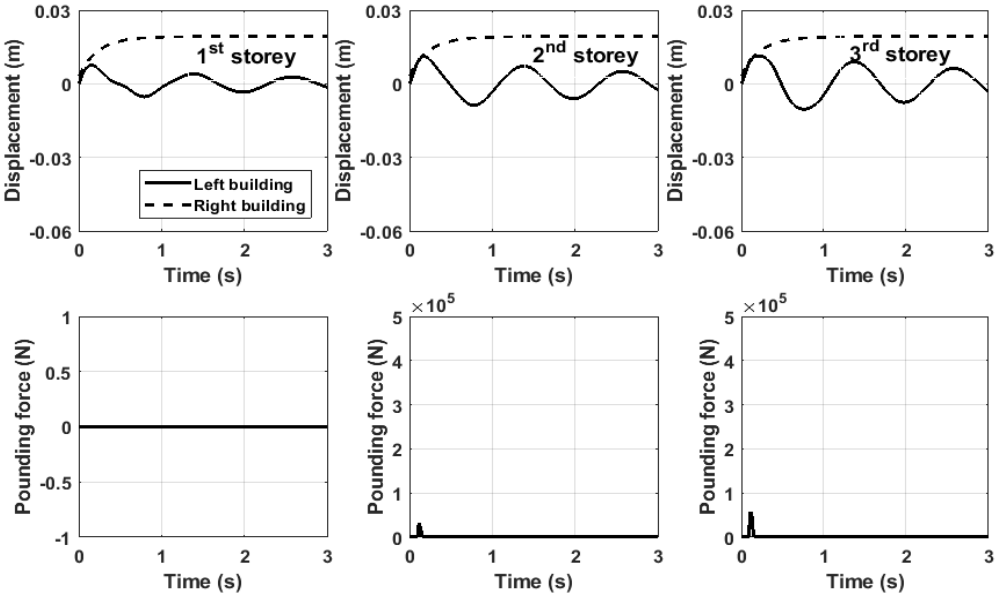

Fig. 7 Displacement and impact force time-histories of adjacent buildings with small separation gap to an explosion near stiff building

causes the higher story levels to collide several times compared with the lower story levels. Notably, the higher stories continue to collide even beyond the time of explosion. It has also been noted that the higher the story level, the higher is the induced peak pounding force value. The heavy and stiff building acts as an abutment or support that prevents the light and flexible building from movement in the direction of hitting, but it only allows movement in the opposite direction. The captured peak pounding force values at the 1st, 2nd, and 3rd stories are 3.9974×10^5 N, 4.3461×10^5 N, and 4.3362×10^5 N, respectively.

The scenarios of occurrence of an explosion near the stiff building for sufficiently and insufficiently separated building models are presented in Figs. 6 and 7, respectively. The plotted curves clearly indicate that the obtained displacements of the stories of the light and flexible buildings show similar patterns with time for the cases without and with collisions. Likewise, the stories of the stiff building produce similar patterns of displacement variation with time for the cases without and with pounding. There is no significant difference in the magnitudes of the induced displacements of the stiff building's stories, even though a small separation gap is introduced to enable collisions between the stories compared with the displacement responses of the state with no collisions. As can be seen from Fig. 6, for adjacent buildings with sufficiently large separation distance to prevent pounding, the displacement responses of the stories of the stiff building remain nearly unchanged with the captured value of 0.016 m, although the explosion occurs in its vicinity. By contrast, the displacement trend of the stories of the flexible building changes with the simulation time. The captured peak values were 0.0078 m, 0.015 m, and 0.020 m for the 1st, 2nd, and 3rd stories, respectively. These obtained peak displacements are lower compared to the state in which the explosion occurs next to the flexible building. The simulation results obtained by setting the separation gap to be sufficiently small so as to ensure collisions between the stories of the neighboring buildings are presented in Fig. 7. The calculated peak displacements of the stories of the flexible building were 0.007 m, 0.0112 m, and 0.0113 m, which show a trend of decrease owing to the occurrence of pounding. The induced peak forces due to collisions at 2nd and 3rd stories are 3.0348×10^4 N and 5.8641×10^4 N, respectively, which are lower than those when an explosion occurs near the flexible building. Only the higher stories come into contact owing to the effect of an explosion near the stiff building. The first peak impact force occurs immediately after the explosion. Moreover, the location of the explosion next to the stiff building causes the higher story levels come into contact only once. The lower stories do not come into contact at all.

7.2 Effect of gap size

The influence of the separation distance between the adjacent multi-story building models was examined by using the dynamic explosive load presented in Fig. 3(a) to dynamically excite the neighboring models as the separation distance was varied from 0 to 10 cm. Fig. 8 presents the peak responses of the three-story models under the previously described dynamic blast load next to the light and flexible building versus the width of the separation gap. The simulation results indicate that in general, as the separation gap increases, the induced peak pounding forces decrease. Wider separation gaps are required between the higher stories as compared to those between the lower stories to prevent collisions between the buildings. The peak displacements of the superstructure of the flexible building show a decreasing trend up to a certain separation gap value, followed by an increase trend before producing nearly unchanged displacement response values as the separation gap increases to prevent collisions between stories. The figure shows the insignificant effect of the

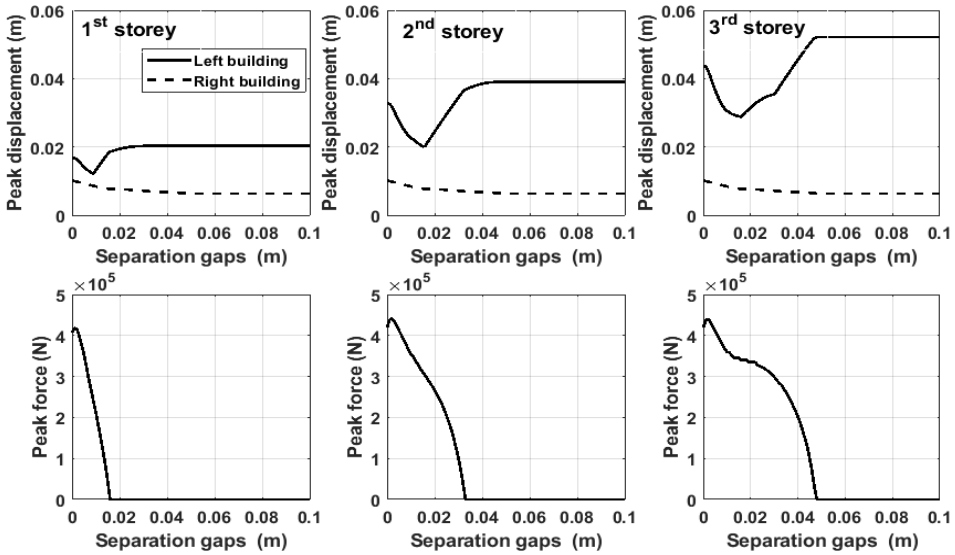

Fig. 8 Peak displacements of stories and corresponding peak impact forces against gap distances to an explosion near flexible building

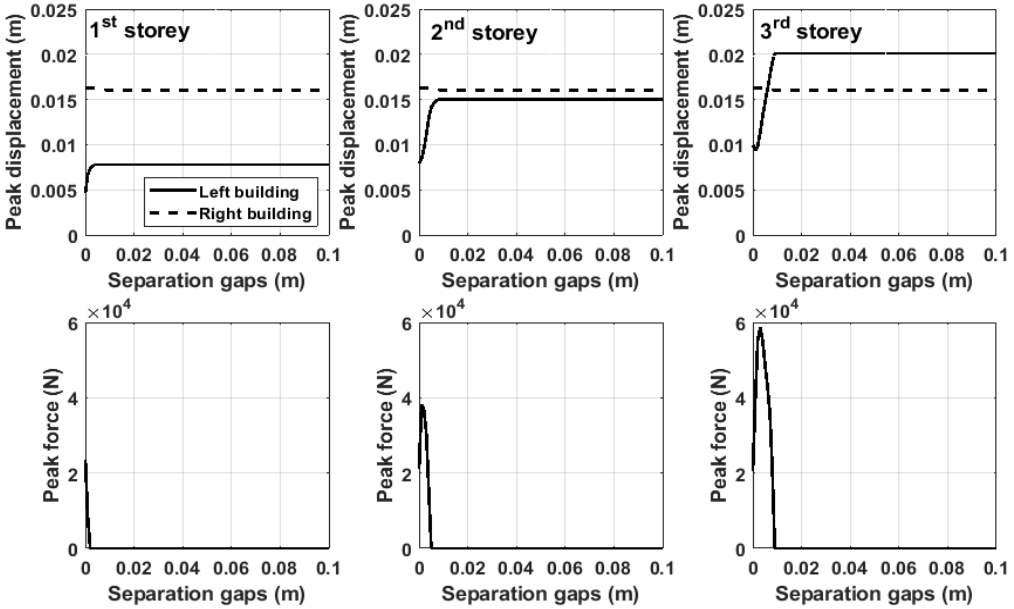

Fig. 9 Peak displacements of stories and corresponding peak impact forces against gap distances to an explosion near stiff building

collisions on the obtained peak displacement responses of the stiff building's stories, where almost all the stories produce similar peak displacement responses for all considered separation distances.

Change in the obtained maximum responses in terms of the displacements of the stories of the flexible and stiff buildings and the corresponding peak forces due to collisions with variation in separation distances under blast load near the right and stiff building are presented in Fig. 9. As can be seen from the figure, collisions occur only when the separation gaps are very small. In addition, collisions between higher stories produce higher peak pounding forces than those induced at lower stories. The figure shows that the displacements of the stories under the applied dynamic blast load are insignificantly influenced by variations in gap size, except at very low values of the separation gap. The peak displacements of the stories of the flexible building change suddenly at very small separation gaps, which corresponds to collisions between the neighboring structures.

7.3 Damage response

The damage model developed by Park-Ang is utilized herein to assess the damage to the adjacent buildings, shown in Fig. 1, with insufficient separation gap. Figs 10 and 11 show the cumulative damage to the two adjacent three-story buildings of equal heights considering the location of the blast load next to the flexible and stiff buildings, respectively. For an explosive load next to the

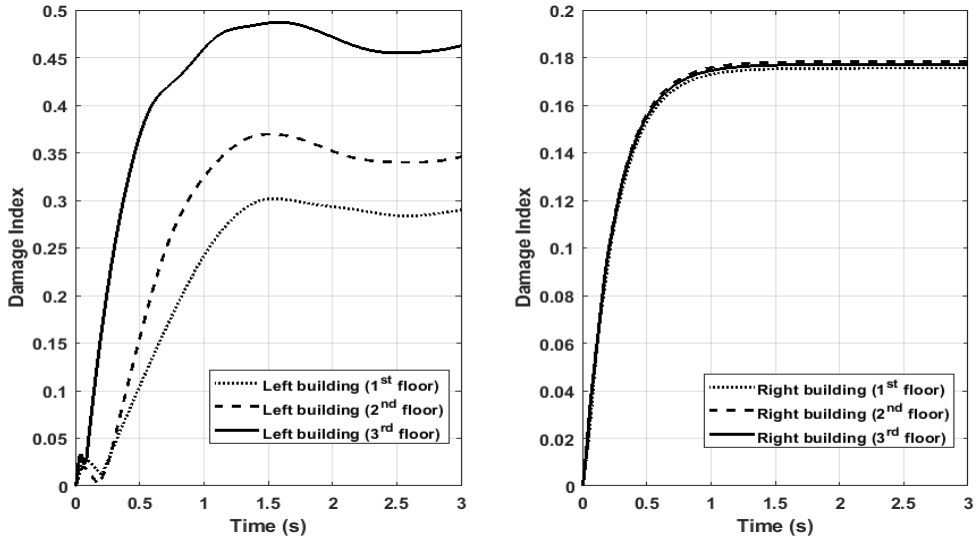

Fig. 10 Damage indices of left and right buildings due to pounding and applied explosive load near left and flexible building

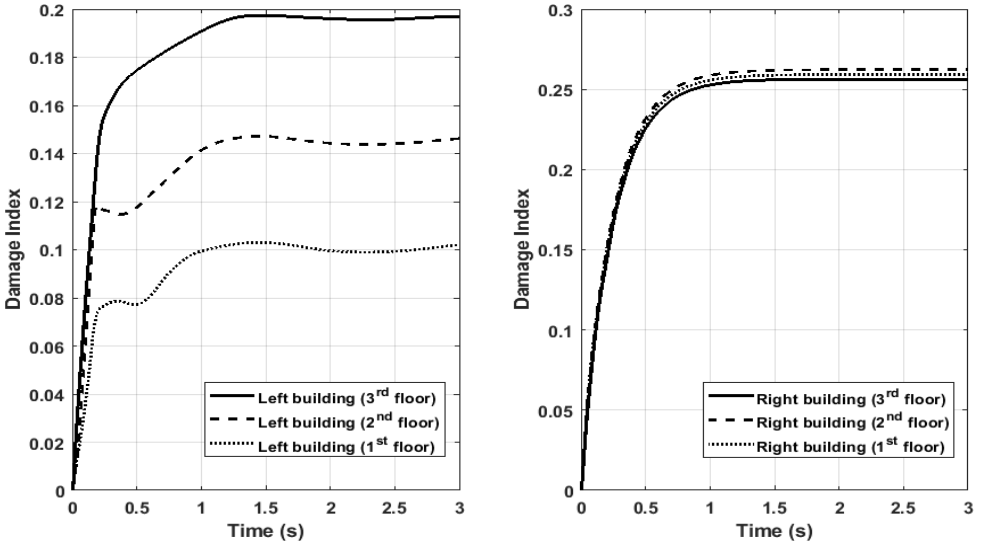

Fig. 11 Damage indices of left and right buildings due to pounding and applied explosive load near right and stiff building

flexible building, damage to the stiff building is less than the damage to the flexible building, as can be seen from Fig. 10. The figure also shows that the higher stories of the flexible buildings are more susceptible to damage. By contrast, the stories of the stiff building provide almost identical damage indices. This study has demonstrated numerically that the extent of damage would be higher for flexible buildings adjacent to stiff buildings of equal heights. The change in the location of the applied dynamic blast load near the stiff building provides an almost similar trend as an explosion near the flexible building. The calculated damage index values of the stories of the stiff building are almost similar and higher compared to the corresponding values of the stories of the flexible building. This can be because the stiff building acts as a barrier protecting the neighboring light and flexible building from the detrimental effects of an explosion near the stiff building.

7.4 Various blast loads

The changes in peak displacements, forces due to collisions, and damage indices at each story level of the adjacent two building models due to variation in peak over static pressure are presented in Figs. 12 and 13; a small separation gap is provided to facilitate collisions between buildings due to an explosion next to the flexible building. The simulation results indicate that the response may increase significantly in case of the stories of the flexible building. Fig. 12 shows the changes in the obtained maximum displacements and the corresponding peak pounding forces against different peak over static pressure values ranging from 44.95 to 312 kPa. As can be seen from the figure, the variation in peak over static pressures significantly affects the displacements of the stories of the light and flexible building. The peak responses of the stories increase with an increase in the applied peak pressure values. The stories at higher levels induce higher peak responses compared to the lower stories. By contrast, the induced deflections of the stories of the stiff building are almost insensitive to variations in the peak pressure values,

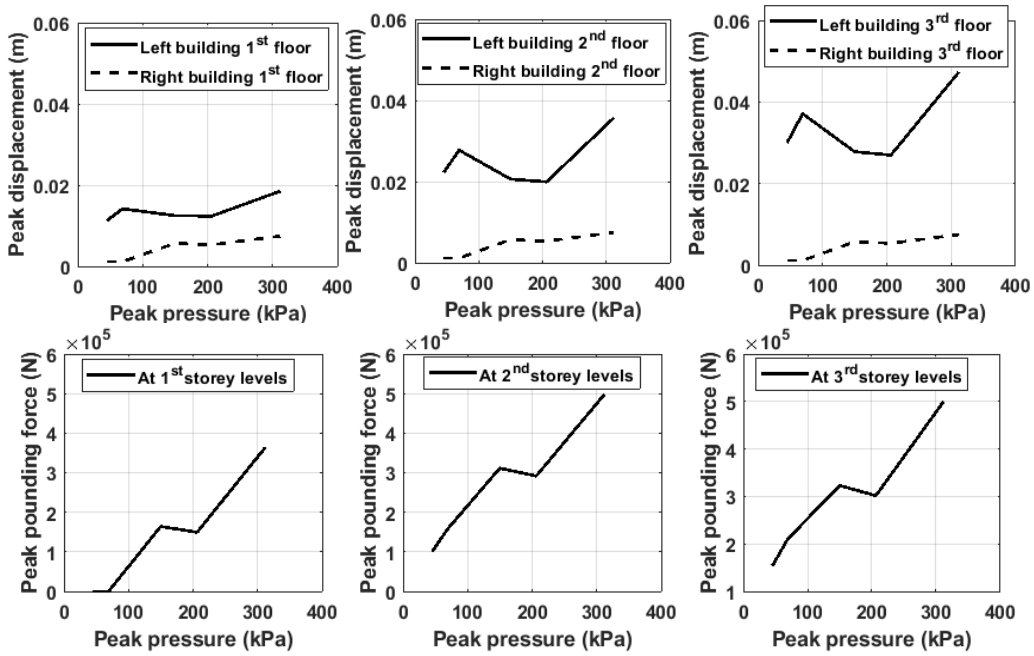

Fig. 12 Variation of peak displacements and peak pounding forces at different peak pressures and applied explosive load near the left and flexible building

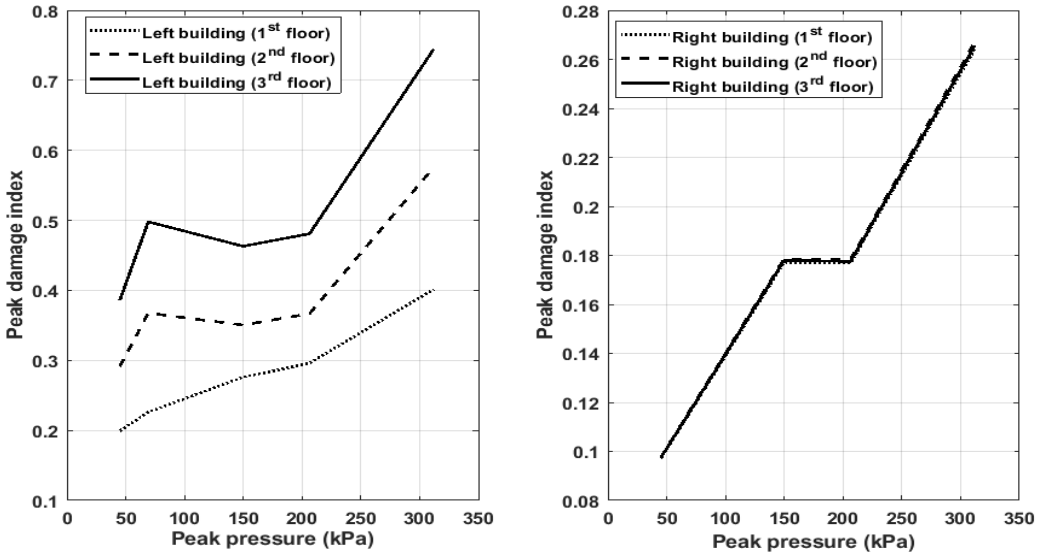

Fig. 13 Variation of peak damage index with different peak pressures for left and right buildings and applied explosive load near the left and flexible building

showing only a slight increase with increasing applied peak over static pressure values.

As expected, the induced peak forces due to collisions increase with increasing peak over static pressure. Collisions at higher story levels show peak pounding forces higher than those induced due to collisions at lower stories. The variation in peak over static pressures against the peak damage index values can be seen in Fig. 13. The captured damage index values of the stories seem to be significantly affected by variations in the peak pressure values. It can be seen from the figure that the higher stories of the left building, the flexible one, are highly susceptible to damage compared to the lower stories. Moreover, the figure clearly indicates that the effect of pressure variation on the change in the damage index values of the stories of the stiff building seems insignificant at the story levels at which the induced peak damage index values appear to be identical. The left building seems to be more vulnerable to explosive loads compared to the right building.

In order to study the effect of flexibility on the induced responses, the superstructures of neighboring two building's models considered herein are assumed to respond as single degree of freedom system (SDOF) with varied fundamental natural period T_n. The remaining dynamic characteristic values in terms of damping and stiffness coefficients c and k respectively can be calculated in terms of the provided mass m, natural period T and damping ration ξ employing the formulas (Harris and Piersol 2002)

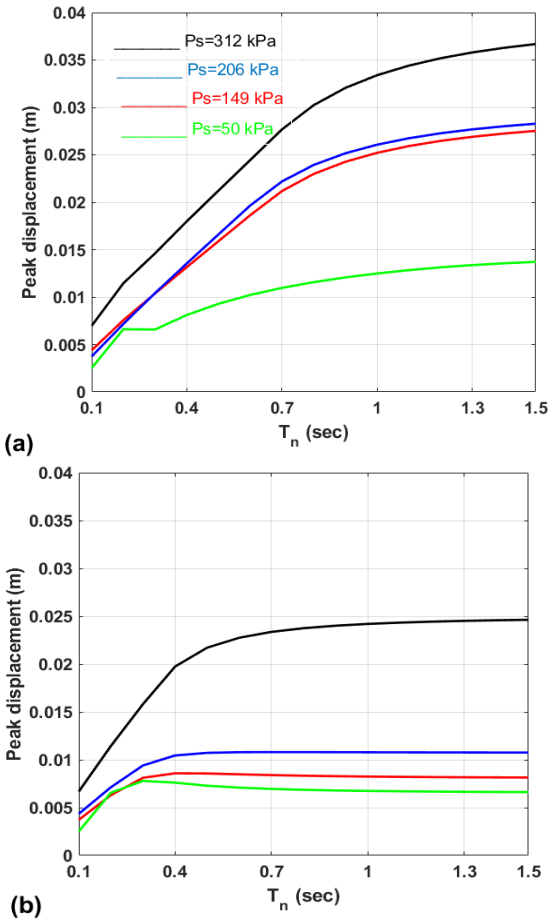

Fig. 14 Variation of the induced peak displacements against natural periods under various blast load near the flexible building (a) without collisions (b) during collisions

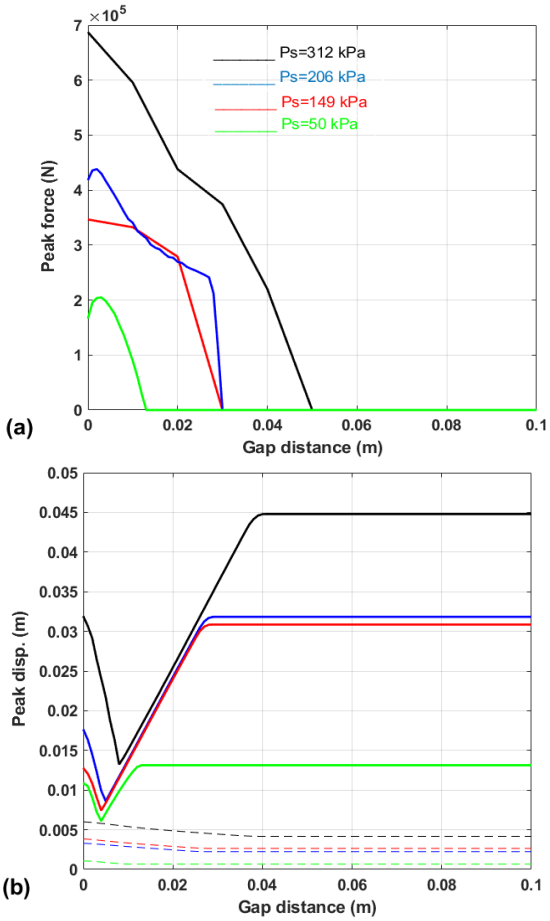

Fig. 15 Variation of the induced (a) peak pounding forces and (b) peak displacements against gap distance under various blast load near the flexible building

$$k^i = \frac{4\pi^2 m^i}{(T^i)^2}; \quad c^i = 2\xi^i\sqrt{k^i m^i} \quad \text{where } i = L, R \qquad (13)$$

Blast load near the light building is considered and the dynamic response in terms of peak displacements against the natural periods of the light building is obtained and presented under the considered various blast loads. Envelops of peak displacement responses are shown in Fig. 14 for without and with collisions under the applied blast loads with different peak over static pressure values. As can be seen from the figure, with the increase in the fundamental period of the building and increase trend in the obtained story displacement can be observed for the case without impacting between the neighboring buildings. However, for the case with impacting, buildings experience an increase trend in the obtained displacements till a specified natural period value. Further increase in the natural periods of the building provides peak displacement responses of nearly unchanged values under all the considered blast loads. This means that responses of sufficiently separated buildings are highly influenced by the flexibility of superstructure. On the other hand, insufficiently separated buildings, i.e., colliding buildings, are influenced slightly by the flexibility of the superstructures after passing a certain natural period value. It can be seen from the figure that, the higher the intensity of the applied blast load is the higher the obtained peak displacement values. The case of collisions provides induced maximum story displacement of lower values compared with the case of no pounding (compare Fig. 14(a) and Fig. 14(b)). comparing Fig. 14(a) and Fig. 14(b) clearly indicates that collision significantly affect the floor peak displacements of the adjacent buildings system.

Simulations of the induced peak pounding forces and peak displacements against separation gaps under various blast loads near the flexible building are presented in Fig. 15. As can be seen from the figure, with the increase in the provided separation distances between the adjacent buildings a decrease trend can be observed in the obtained impacting forces under all the applied dynamic blast loads. Moreover, the higher the applied blast load is the higher the needed separation gap value to prevent pounding between the buildings. In addition, considerable reduce in the obtained peak pounding force values with the decrease in the intensity of the applied blast loads. The obtained peak displacements of the story of the flexible building show a decrease trend up to a certain minimum separation gap value. Passing such a minimum gap value shows an increase trend in peak displacements followed by nearly peak response values with the increase in separation gaps for all the applied various dynamic blast loads. The

displacement responses of the story of stiff building show a slight decrease with the increase of the provided separation distances during collisions and with further increase in the provided gaps the obtained peak displacement responses show almost constant displacement values under all the considered blast loads.

8. Conclusions

The responses of adjacent building models with different dynamic characteristics to localized blast loading are investigated for two scenarios of in-between stand-off-distance. One of the scenarios considers a sufficiently large separation gap to prevent collisions under the applied blast loads. The second scenario allows for collisions between the stories by employing a small separation gap. To obtain a comprehensive understanding of the performance of neighboring buildings under blast loads, two different orientations were simulated in terms of explosion location. The obtained responses of the buildings from the studied scenarios and orientations in terms of deformation, pounding force, and damage index were evaluated. The findings and conclusions are as follows:

- The stiff building produced the lowest deformation compared to the flexible building for separation gaps and explosion locations. In addition, the stories of the stiff buildings remained intact under all considered magnitudes of blast loadings.
- The applied dynamic blast load significantly influenced the displacement response of the stories of the flexible building, but not the stories of the stiff building, especially for an explosion next to the flexible building.
- For insufficiently separated buildings with different dynamic characteristics, the location of the explosion significantly influenced the magnitude and number of impacts of the forces induced by collisions. The scenario with an explosion near the flexible building produced a number of contacts and pounding forces with considerably higher magnitudes than those in the other scenario.
- The considered range of peak pressures significantly influenced the damage level of the stories of the flexible building but not that of the stiff building.
- The induced peak pounding forces were found to be proportional to variations in the peak pressure of the blast loads.
- The higher the stories, the higher the induced damage index of the flexible building, regardless the location of the explosion. However, the level of damage of the stories of the stiff building seemed to be insignificantly affected by the explosion location.

References

Anagnostopoulos, S.A. and Spiliopoulos, K.V. (1992), "An investigation of earthquake induced pounding between adjacent buildings", *Earthq. Eng. Struct. Dyn.*, **21**(4), 289-302. https://doi.org/10.1002/eqe.4290210402.

Baker, W.E. (1973), *Explosions in Air*, Univ. of Texas Press, Austin TX USA.

Bao, X.L. and Li, B. (2010), "Residual strength of blast damaged reinforced concrete columns", *Int. J. Impact Eng.*, **37**(3), 295-308. https://doi.org/10.1016/j.ijimpeng.2009.04.003.

Chau, K.T. and Wei, X.X. (2001), "Pounding of structures modelled as non-linear impacts of two oscillators", *Earthq. Eng. Struct. Dyn.*, **30**, 633-651. https://doi.org/10.1002/eqe.27.

Cosenza, E., Manfredi, G. and Ramasco, R. (1993), "The use of damage functionals in earthquake resistant design: a comparison among different procedures", *Earthq. Eng. Struct. Dyn.*, **22**(10), 855-868.

Dyer, J., Raibagkar, A., Kolbe, M. and Salzano, E. (2012), "Blast damage consideration for horizontal pressure vessel and potential for domino effect", *Chem. Eng. Tran.*, **26**(1), 87-92. https://doi.org/10.3303/CET1226015.

Elsanadedy, H.M., Almusallam, T.H., Alharbi, Y.R., Al-Salloum, Y.A. and Abbas, H. (2014), "Progressive collapse potential of a typical steel building due to blast attacks", *J. Constr. Steel Res.*, **101**, 143-157. https://doi.org/10.1016/j.jcsr.2014.05.005.

Harris, C.M. and Piersol, A.G. (2002), *Harris' Shock and Vibration Handbook*, Eds. C.M. Harris and A.G. Piersol, McGraw-Hill publishing, New York.

Jain, S., Tiwari, R., Chakraborty, T. and Matsagar, V. (2015), "Dynamic response of reinforced concrete wall under blast load", *Ind. Concrete J.*, **89**(8), 27-41.

Jankowski, R. (2005), "Non-linear viscoelastic modelling of earthquake-induced structural pounding", *Earthq. Eng. Struct. Dyn.*, **34**(6), 595-611. https://doi.org/10.1002/eqe.434.

Jankowski, R. (2006), "Analytical expression between the impact damping ratio and the coefficient of restitution in the non-linear viscoelastic model of structural pounding", *Earthq. Eng. Struct. Dyn.*, **35**(4), 517-524. https://doi.org/10.1002/eqe.537.

Kingery, C. and Bulmash, G. (1984), "Airblast parameters from TNT spherical air burst and hemispherical surface burst", Tech. Rep. ARBL-TR-02555, US Army BRL, Aberdeen Proving Ground, Maryland, USA.

Kumar, M., Matsagar, V. and Rap, K. (2010), "Blast load on semi-buried structures with soil-structure interaction", *Proceedings of the IMPLAST Conference*, October.

Lopez-Garcia, D. and Soong, T.T. (2009), "Assessment of the separation necessary to prevent seismic pounding between linear structural systems", *Prob. Eng. Mech.*, **24**(2), 210-223. https://doi.org/10.1016/j.probengmech.2008.06.002.

Mahmoud, S. (2014), "Blast loads induced response and the associated damage of buildings considering SSI", *Earthq. Struct.*, **7**(3), 349-365. https://doi.org/10.12989/eas.2014.7.3.349.

Mahmoud, S. (2016), "Dynamic response of adjacent buildings under explosive loads", *Arab. J. Sci. Eng.*, **41**(10), 4007-4018. ttps://doi.org/10.1007/s13369-016-2086-6.

Maison, B.F. and Kasai, K. (1992), "Dynamics of pounding when two buildings collide", *Earthq. Eng. Struct. Dyn.*, **21**(9), 771-786. https://doi.org/10.1002/eqe.4290210903.

Park, Y.J. and Ang, A.H. (1985), "Mechanistic seismic damage model for reinforced concrete", *J. Struct. Eng.*, ASCE, **111**(4), 722-739. https://doi.org/10.1061/(ASCE)0733-9445(1985)111:4(722).

Powell, G.H. and Allahabadi, R. (1988), "Seismic damage prediction by deterministic methods: concepts and procedures", *Earthq. Eng. Struct. Dyn.*, **16**(5), 719-734. https://doi.org/10.1002/eqe.4290160507.

Smith, P.D. and Hetherington, J.G. (1984), *Blast and Ballistic Loading of Structures*, Laxton's.

Yan, B., Liu, F., Song, D.Y. and Jiang, Z.G. (2015), "Numerical study on damage mechanism of RC beams under close-in blast loading", *Eng. Fail. Anal.*, **51**, 9-19. https://doi.org/10.1016/j.engfailanal.2015.02.007.

Yao, S.J., Zhang, D., Lu, F.Y., Wang, W. and Chen, X.G. (2016), "Damage features and dynamic response of RC beams under blast", *Eng. Fail. Anal.*, **62**(4), 103-111. https://doi.org/10.1016/j.engfailanal.2015.12.001.

Zhang, D., Yao, S., Lu, F., Chen, X., Lin, G., Wang, W. and Lin, Y. (2013), "Experimental study on scaling of RC beams under close-in blast loading", *Eng. Fail. Anal*., **33**, 497-504. https://doi.org/10.1016/j.engfailanal.2013.06.020.

CC